Stem Cell Rev and Rep (2011) 7:331–341
DOI 10.1007/s12015-010-9209-3

A Cyclic AMP Analog, 8-Br-cAMP, Enhances the Induction of Pluripotency in Human Fibroblast Cells

Ying Wang · James Adjaye

Published online: 1 December 2010

Abstract Somatic cells can be reprogrammed into induced pluripotent stem (iPS) cells by ectopic expression of four transcription factors. However, the efficiency of human iPS cell generation is extremely low and therefore elucidating the mechanisms underlying cellular reprogramming is of prime importance. We demonstrate that 8-Bromoadenosine 3′, 5′-cyclic monophosphate (8-Br-cAMP) improves the reprogramming efficiency of human neonatal foreskin fibroblast (HFF1) cells transduced with the four transcription factors by 2-fold. The combination of 8-Br-cAMP and VPA synergistically increases the efficiency to 6.5-fold. The effect of 8-Br-cAMP or VPA may in part be due to the up-regulation of cytokine-related and inflammatory pathways. Remarkably, the synergistic effect of 8-Br-cAMP and VPA on cellular reprogramming may be due to the transient decrease of p53 protein during the early stages of reprogramming. However, it could also be due to additional differentially regulated genes and pathways such as the up-regulation of cytokine-related, inflammatory pathways and self-renewal supporting gene, namely cyclin-encoding *CCND2*, and the associated genes *CCNA1* and *CCNE1*. Conversely, we also see the down-regulation of the p53 (*CCNB2, GTSE1*, *SERPINE1*) and cell cycle (*PLK1*, *CCNB2*) pathways. Our data demonstrates that a cyclic AMP analog, 8-Br-cAMP, enhances the efficiency of cellular reprogramming. In addition, 8-Br-cAMP and VPA have a synergistic effect on cellular reprogramming, which may be in part due to the transient down-regulation of the p53 signaling pathway during the early stages of reprogramming.

Keywords Induced pluripotent stem cells · Embryonic stem cells · Pluripotency · 8-Br-cAMP · VPA · p53 · Cell cycle

Introduction

Mouse or human somatic cells can be reprogrammed into a pluripotent state by ectopic expression two sets of four defined transcription factors, namely, OCT4, SOX2, KLF4, and c-MYC or OCT4, SOX2, NANOG, and LIN28 [1–4]. These induced pluripotent stem (iPS) cells exhibit characteristics similar to those of embryonic stem (ES) cells, for example, with respect to their transcriptome, epigenetic states, self-renewal and pluripotency. Furthermore, iPS cells possess enormous potential for basic research on developmental biology, modeling of diseases, toxicology, drug screening and cell replacement therapies [5–17].

The reprogramming protocol is very robust and reproducible, however, many problems need to be resolved before human iPS cells can be used for routine regenerative therapies. One of the problems is the efficiency of reprogramming human somatic cells to iPS cells is extremely low, ranging from 0.0095% to 0.02% [3, 4]. A preferable method is the use of small molecules to improve the efficiency of iPS cell generation. A number of laboratories have identified small molecules that can

Electronic supplementary material The online version of this article (doi:10.1007/s12015-010-9209-3) contains supplementary material, which is available to authorized users.

Y. Wang · J. Adjaye (✉)
Department of Vertebrate Genomics, Molecular Embryology and Aging Group, Max Planck Institute for Molecular Genetics, Ihnestrasse 63-73,
14195, Berlin, Germany
e-mail: adjaye@molgen.mpg.de
URL: http://www.molgen.mpg.de/~molemb/

J. Adjaye
The Stem Cell Unit, Department of Anatomy, College of Medicine, King Saud University,
P.O. Box 2925, Riyadh 11461, Saudi Arabia

enhance reprogramming efficiencies of mouse iPS cell generation, including 5-azacytidine, valproic acid (VPA, a histone deacetylase inhibitor), TSA, SAHA, BIX 01294, BIX 01294 plus BayK8644 or RG108, and vitamin C [18–23]. In contrast, only three laboratories have reported several small molecules capable of significantly increasing the derivation of human iPS cells. An important progress was made by Huangfu et al. demonstrating that VPA significantly enhanced the efficiency of deriving human iPS cells from neonatal foreskin or dermal fibroblasts employing only two transcription factors, namely, OCT4 and SOX2 [24]. Another approach, which involves the inactivation of TGFβ and MEK-ERK pathways using inhibitors of the respective receptors, SB431542 and PD0325901, in combination with thiazovivin, improved the efficiency of reprogramming by >200 fold [25]. Furthermore, it has been demonstrated that vitamin C significantly enhanced the efficiency of human iPS cell generation [22].

Based on our previous studies on OCT4-dependent transcriptional networks regulating self-renewal in human ES cells [26], we identified genes within cyclic AMP-dependent pathways to be differentially expressed upon ablation of OCT4 function. With this in mind, we screened available literature for small molecules capable of modulating cyclic AMP-dependent pathways.

In this study, we demonstrate that 8-Br-cAMP can enhance the reprogramming efficiency of human neonatal foreskin fibroblast (HFF1) cells transduced with OCT4, SOX2, KLF4, and c-MYC by 2-fold. In addition, the combination of 8-Br-cAMP and VPA has a synergistic effect on improving the reprogramming efficiency (6.5-fold). Microarray analysis revealed that cytokine-related and inflammatory pathways were up-regulated in four factor-transduced HFF1 cells treated with 8-Br-cAMP, VPA or both. Remarkably, the combination of 8-Br-cAMP and VPA induced a transient decrease in the protein expression level of p53 during the early stages of reprogramming. It has been shown that siRNA-mediated ablation of p53 function significantly improved the efficiency of reprogramming [27–32]. Additionally, the synergistic effect of 8-Br-cAMP and VPA on reprogramming may be in part due to additional differentially regulated genes and pathways such as up-regulation of the cytokine-related, inflammatory pathways and the self-renewal supporting cyclin-encoding gene *CCND2*, in conjunction with *CCNA1* and *CCNE1*, and down-regulation of p53 (*CCNB2, GTSE1*, *SERPINE1*) and cell cycle (*PLK1, CCNB2*) pathways.

Materials and Methods

Cell Culture

Human fetal foreskin fibroblast cells (HFF1, ATCC, #ATCCSCRC-1041, http://www.atcc.org) and Phoenix™ Ampho cells (Orbigen, Inc., #RVC-10001, http://www.orbigen.com) were maintained in Dulbecco's modified eagle medium (DMEM, Invitrogen, Carlsbad, CA, http://www.invitrogen.com) containing 10% fetal bovine serum (Invitrogen) and 0.5% penicillin and streptomycin (Invitrogen). Human ES and iPS cells were maintained on irradiated mouse embryonic fibroblasts (MEFs) in KnockOut DMEM (Invitrogen) supplemented with 20% KnockOut serum replacement (Invitrogen), 0.1 mM non-essential amino acids (Invitrogen), 1 mM L-glutamine (Invitrogen), 0.1 mM β-mercaptoethanol (Invitrogen), 0.5% penicillin and streptomycin, and 4 ng/ml basic fibroblast growth factor (bFGF, Invitrogen). For passaging, iPS cells were split 1 : 3 using 1 mg/ml collagenase IV (Invitrogen). For feeder-free culture, iPS cells were seeded on Matrigel (Becton Dickinson, Franklin Lakes, NJ, http://www.bd.com)-coated plates in MEF-conditioned medium supplemented with 4 ng/ml bFGF.

Retroviral Production and Generation of iPS Cells

pMXs-based retroviral vectors each encoding the transcription factors *OCT4*, *SOX2*, *KLF4*, and *c-MYC* were transfected into Phoenix™ Ampho cells using Fugene transfection reagent (Roche Diagnostics, Basel, Switzerland, http://www.roche-applied-science.com). Viral supernatants were collected 48 and 72 hours post-transduction. For the generation of iPS cells, we first seeded HFF1 cells onto plates. 24 hours later, HFF1 cells were incubated with a 1:1:1:1 mixture of viral supernatants supplemented with 4 ug/ml polybrene (Sigma, St. Louis, http://www.sigmaaldrich.com) and we then centrifuged the entire plates at 800 rcf for 99 min using the Eppendorf centrifuge 5810R. After 24 hours, the cells were infected once more repeating the same procedure as above. Twenty four hours thereafter, the infected cells were re-seeded onto irradiated MEF feeder layers (1×10^4 cells/well, 12-well plate). On the following day, the medium was changed to human ES cell culture medium and supplemented with 0.1 / 0.5 mM 8-Br-cAMP (Biaffin GmbH & Co KG, Kassel, Germany, http://www.biaffin.com, dissolved in ddH_2O), 0.5 mM VPA (CALBIOCHEM, San Diego, http://www.emdbiosciences.com, dissolved in ddH_2O), 0.1 mM 8-Br-cAMP plus 0.5 mM VPA or 0.5 mM 8-Br-cAMP plus 0.5 mM VPA. The medium was changed every other day. The chemical treatment was continued for 1 week. 10 days post-transduction, the medium was replaced with MEF-conditioned medium supplemented with 4 ng/ml bFGF. On day 30–35 post-transduction, the cells were fixed to analyse the number of NANOG positive ES cell-like colonies. To establish iPS cell lines, human ES cell-like colonies were picked, mechanically dissociated to small clumps then transferred onto irradiated MEF feeder layers in human ES cell medium for further expansion.

Alkaline Phosphatase Staining and Immunofluorescence Staining

Alkaline phosphatase staining was performed using an alkaline phosphatase detection kit (Millipore, Billerica, MA, http://www.millipore.com) according to the manufacturer's protocol. For immunofluorescence staining, the cells were fixed in 4% paraformaldehyde in PBS for 20 min, permeabilized by 0.1% Triton X-100 (Sigma) for 10 min at room temperature and blocked with 10% chicken serum for 30 min. Subsequently, the cells were incubated with the primary antibodies overnight at 4°C. The primary antibodies include monoclonal antibodies against OCT4 (1:100, Santa Crutz Biotechnology Inc., Santa Cruz, CA, http://www.scbt.com, #sc-8629), SOX2 (1:100, Santa Crutz Biotechnology Inc., #sc-17320), NANOG (1:500, Abcam, Cambridge, U.K., http://www.abcam.com, #ab62734), SSEA1, SSEA4, TRA-1-60, and TRA-1-81 from the ES cell characterization tool (all 1:500, Millipore, #SCR004), SSEA-3 (1:500, Abcam, #ab16286), α-FETOPROTEIN (AFP, 1:50, Sigma, #WH0000174M1), SOX17 (1:50, R&D Systems, Inc., http://www.rndsystems.com, #AF1924), α-SMOOTH MUSCLE ACTIN (SMA, 1:100, DakoCytomation, Glostrup, Denmark, http://www.dakocytomation.com, #M0851), BRACHYURY (1:50, R&D Systems, Inc., #AF2085), βIII-TUBULIN (1:400, Sigma, #T8660) and PAX6 (1:300, Covance, http://www.covance.com, #PRB-278P). Secondary antibodies used were conjugated with either Alexa 488 or Alexa 594 (1:300, Invitrogen, #A11001, A11055, A21201, A21468, A11005, A21442), which were incubated with the cells for 1 hour at room temperature in the dark. Samples were analyzed on a Zeiss Fluorescence microscope.

In Vitro Differentiation

iPS cells were cultured in feeder-free conditions and then harvested using 1 mg/ml collagenase IV. Small clumps were transferred to low attachment dishes (Corning Inc., Corning, NY, http://www.corning.com) in KnockOut DMEM supplemented with 20% KnockOut serum replacement, 0.1 mM non-essential amino acids, 1 mM L-glutamine, 0.1 mM β-mercaptoethanol, and 0.5% penicillin and streptomycin. The medium was changed every other day. After 7 days of continuous growth in suspension culture, the clumps formed embryoid bodies (EBs). These EBs were transferred to gelatin-coated plates and cultured in the same medium for further 5–10 days.

Teratoma Formation

iPS cells were cultured in feeder-free condition and then collected using 1 mg/ml collagenase IV. Approximately one million cells were subcutaneously injected into NOD.Cg-Prkdcscid Il2rgtm1Wjl/SzJ mice, commonly known as NOD scid gamma. After two months, induced teratomas were dissected, fixed in 4% paraformaldehyde, and embedded in paraffin. Paraffin-embedded tissues were then sectioned and stained with hematoxylin and eosin.

Karyotyping

Standard G-banding chromosome analysis was performed at the Human Genetic Center of Berlin. For each sample, 20 metaphases were counted and 12 karyograms were analyzed.

DNA Fingerprinting

Tandem repeat analysis was carried out using the same protocol as previously described [33]. Briefly, genomic DNA was isolated using the FlexiGene DNA kit (Qiagen, Hilden, Germany, http://www.qiagen.com) and PCR was employed to detect genomic intervals containing variable numbers of tandem repeats. A total of 50 ng of DNA was amplified at 94°C for 1 min, 55°C for 1 min, and 72°C for 1 min for a total of 40 cycles using a Dyad thermal cycler (Bio-Rad, Hercules, CA, http://www.bio-rad.com) and then amplicons resolved on 3% agarose gel. Primer sequences are described in Supplemental Table S6.

Microarray-Based Gene Expression Analysis

Total RNA was extracted using the MiniRNeasy Kit (Qiagen) according to the manufacturer's instructions and quality checked by Nanodrop analysis (Nanodrop Technologies, Wilmington, DE, USA, http://www.nanodrop.com). Approximately 500 ng of DNase treated RNA served as input for biotin-labeled cRNA production using a linear amplification kit (Ambion, Austin, TX, http://www.ambion.com). Hybridizations, washing, Cy3-streptavidin staining, and scanning were performed on the Illumina BeadStation 500 platform (Illumina, San Diego, CA, http://www.illumina.com) according to manufacturer's instruction. cRNA samples were hybridized onto Illumina human-8 BeadChips version 3. All basic expression data analysis was carried out using the BeadStudio software 3.0. Raw data were background-subtracted and normalized using the "rank invariant" algorithm and then filtered for significant expression on the basis of negative control beads.

For correlation coefficient analysis and the generation of Venn diagrams, detected gene expression was defined by a Detection P Value <0.01 as output by BeadStudio.

For differential gene expression analyses, genes had to be at least 1.5 fold up- or down-regulated in a group-wise comparison, to be considered significantly differentially expressed.

Pathway analysis was performed according to Gene Ontology terms on the basis of the DAVID platform version 6.7 (http://david.abcc.ncifcrf.gov) using GenBank ENTREZ_GENE_IDs represented by the corresponding chip oligonucleotides as input. The Homo Sapiens species was selected as background. DAVID was executed with default parameter settings on the 19th of April 2010.

Quantitative Real-Time PCR

Total RNA was extracted using MiniRNeasy Kit (Qiagen) according to the manufacturer's instructions. 1 ug of total RNA was used for Oligo $(dT)_{20}$-primed reverse transcription. Quantitative Real-Time PCR was performed with Platinum SYBR Green quantitative PCR Supermix UDG (Applied Biosystems, Foster City, CA, http://www.appliedbiosystems.com). Reactions were carried out on the ABI PRISM 7900HT Sequence Detection System (Applied Biosystems) as previously described [34]. Triplicate amplifications were carried out for each target gene with three wells serving as negative controls. Quantification was performed using the comparative Ct method (ABI instruction manual) normalized with the housekeeping genes *GAPDH* and presented as a percentage of biological controls. Primer sequences are described in Supplemental Table S6.

Western Blotting

Total cell protein extracts were obtained employing a modified RIPA buffer (50 mM Tris pH 7.4, 100 mM NaCl, 10 mM EDTA, 1 mM PMSF, 1% IGEPAL) supplemented with a complete protease inhibitor cocktail (Roche Diagnostics) prior to use. Protein concentration was determined according to the Bradford method. Proteins (20 ug) were resolved by electrophoresis on a 10% sodium dodecyl sulfate-polyacrylamide gel and transferred to nitrocellulose membrane (GE Healthcare Life Sciences, Piscataway, NJ, http://www.gelifesciences.com). The membrane was incubated with primary antibody at 4°C overnight. Primary antibodies include anti-p53 (1:1,000, Cell Signaling, Danvers, MA, http://www.cellsignal.com, #9282) and anti-GAPDH (1:5,000, Ambion, #4300). After washing with TBST, the membrane was respectively incubated with secondary antibody ECL anti-rabbit IgG or anti-mouse IgG (GE Healthcare Life Sciences) for 1 hour at room temperature. Signals were detected with ECL plus western blotting detection system (GE Healthcare Life Sciences).

Statistical Analysis

Comparisons between two groups were made using two-tailed unpaired student's *t*-test. Data represent the mean of three experiments unless otherwise noted and are expressed as mean and standard deviation. P values of <0.05 were considered statistically significant.

Results

8-Br-cAMP Enhances the Efficiency of Inducing Pluripotency in Human Fibroblast Cells

Viral transduction protocols were first optimized in HFF1 cells using viral particles generated from a pMXs-GFP reporter. HFF1 cells were then infected with distinct concentrations of pMXs-GFP retrovirus. We observed that transduction efficiencies improved as the concentration of retrovirus increased. However, the majority of HFF1 cells died when the highest concentration of retrovirus were applied. We chose the concentration of retrovirus with the highest transduction efficiency and without obvious cell death as an optimized protocol. The transduction efficiency was more than 60% (Supplemental Fig. S1). The same concentration was also used for transductions with the OCT4, SOX2, KLF4, and c-MYC retrovirus.

A time schedule of iPS cell generation is depicted in Fig. 1a. HFF1 cells were transduced twice with retroviral vectors each encoding *OCT4*, *SOX2*, *KLF4*, and *c-MYC* and then supplemented with 0.1/0.5 mM 8-Br-cAMP, 0.5 mM VPA, 0.1 mM 8-Br-cAMP plus 0.5 mM VPA or 0.5 mM 8-Br-cAMP plus 0.5 mM VPA for 1 week (no supplementation served as a negative control, whilst VPA as a positive control). Approximately 30–35 days post-transduction, we assessed the number of colonies that were similar to human ES cells with respect to morphology and simultaneously positive for NANOG as shown by immunofluorescence staining. We deduced that 0.1/0.5 mM 8-Br-cAMP enhanced the number of NANOG positive ES cell-like colonies by approximately 2-fold as compared to the negative control. Additionally, the combination of 0.1 mM 8-Br-cAMP and 0.5 mM VPA had a synergistic effect, increasing the number of NANOG positive ES cell-like colonies by 6.5-fold. However, the combination of 0.5 mM 8-Br-cAMP and 0.5 mM VPA did not significantly increase the number of NANOG positive ES cell-like colonies as the combination of 0.1 mM 8-Br-cAMP and 0.5 mM VPA (Fig. 1b and c). We observed that there were more dead cells after treatment with the combination of 0.5 mM 8-Br-cAMP and 0.5 mM VPA (data not shown). Treatment of HFF1 cells with 0.1 mM 8-Br-cAMP did not lead to altered proliferation rates. In contrast, 0.5 mM VPA decreased the proliferation rates at day 4 and 5. 0.1 mM 8-Br-cAMP plus 0.5 mM VPA inhibited the rates of proliferation at day 3, 4 and 5 (Supplemental Fig. S2).

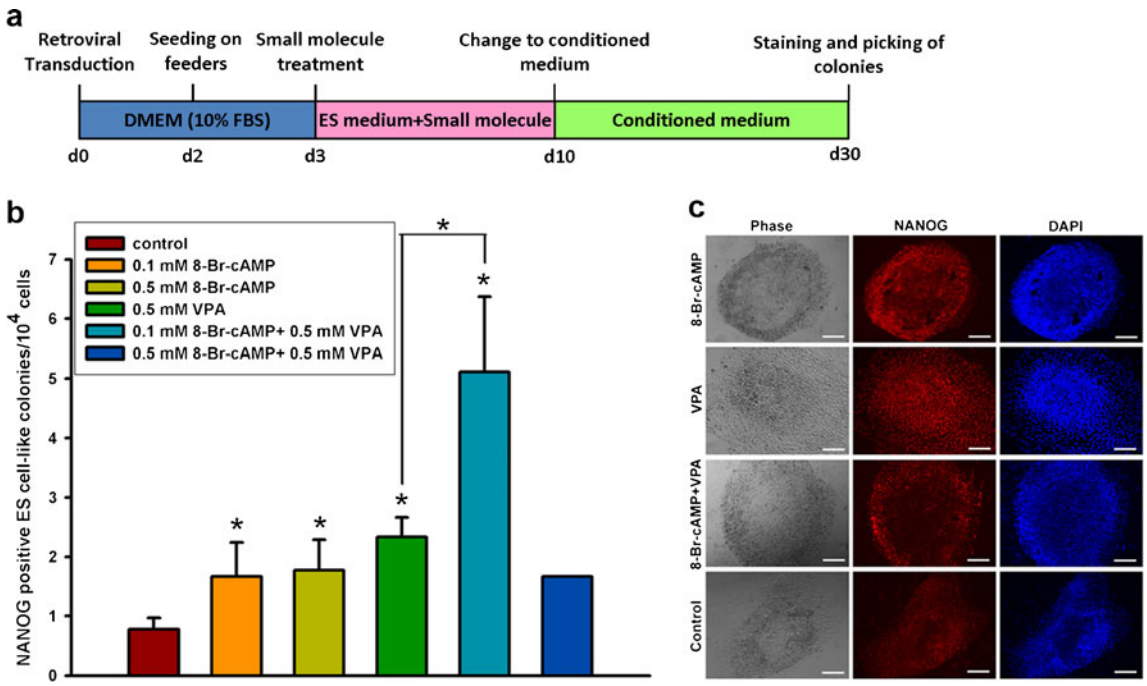

Fig. 1 8-Br-cAMP enhances the efficiency of inducing pluripotency in human fibroblast cells. **a** The time schedule of induced pluripotent stem (iPS) cell generation treated with the indicated small molecules. **b** The average number of NANOG positive embryonic stem (ES) cell-like colonies formed from 1×10^4 of four factor-transduced cells treated with the indicated small molecules in three independent experiments. *P* values <0.05 are indicated by an asterisk. **c** Colonies were similar to human ES cell colony morphology and simultaneously positive for NANOG detected by immunofluorescence staining on day 30–35 post-transduction. Scale bars represent 100 μm

iPS Cells Derived from 8-Br-cAMP-Treated Cells Express Pluripotency Markers and Have a Normal Karyotype

Three ES cell-like colonies derived from 8-Br-cAMP-treated cells were picked and continuously expanded on irradiated mouse embryonic fibroblast (MEF) feeder cells in human ES cell culture medium for 30 passages. All iPS cells were similar to human ES cells in their morphology and expression of pluripotency markers, including alkaline phosphatase (AP), OCT4, SOX2, NANOG, SSEA-3, SSEA-4, TRA-1-60, and TRA-1-81 (Fig. 2a). We also detected the expression of pluripotency-associated genes by quantitative Real-Time PCR analysis. The expression of *OCT4*, *SOX2*, *NANOG*, *GDF3*, *DPPA4* and *CRIPTO* in the three iPS cell lines was remarkably higher than those in their parental cell line, HFF1, and comparable to the human ES cells (H1) (Fig. 2b). The expression of *KLF4* and *c-MYC* was not markedly distinct from HFF1 or H1 cells (Fig. 2b). In addition, the derived iPS cells exhibited a normal diploid male chromosomal content (Supplemental Fig. S3). DNA fingerprinting analysis showed the iPS cell lines were derived from HFF1 cells, thus excluding the possibility that they arose from contaminating human ES (H1 and H9) cells (Supplemental Fig. S4).

The Transcriptomes of iPS Cells are Similar to that of ES Cells

Hierarchical clustering analysis revealed that the transcriptomes of iPS cells and ES cells (H1) were similar and both distinct from HFF1 cells (Fig. 2c). A heatmap generated from the transcriptomes of iPS, ES (H1) and HFF1 cells, revealed four distinct clusters (Fig. 2b). Cluster 1 and 2 consisted of HFF1-enriched genes (*DCN, CNTN3, PRRX1, PSG5*). Cluster 3 and 4 consisted of genes enriched in pluripotent cells (*OCT4, NANOG, SOX2, DPPA4*). The description of genes within each cluster is presented in Supplemental Table S1. Pearson correlation co-efficient analysis showed that iPS cells resemble human ES cells (R^2=0.8797–0.8903). The transcriptomes of distinct iPS cells are similar (R^2=0.9128–0.9252) and distinct (R^2=0.6371–0.6598) from HFF1 cells from which they were derived (Fig. 2d).

Demonstration of Pluripotency *In Vitro* and *In Vivo*

The three iPS cell lines formed embryoid bodies (EBs) in suspension culture and further differentiated into derivatives of the three embryonic germ layers (endoderm, mesoderm, and ectoderm) in adherent culture as shown by

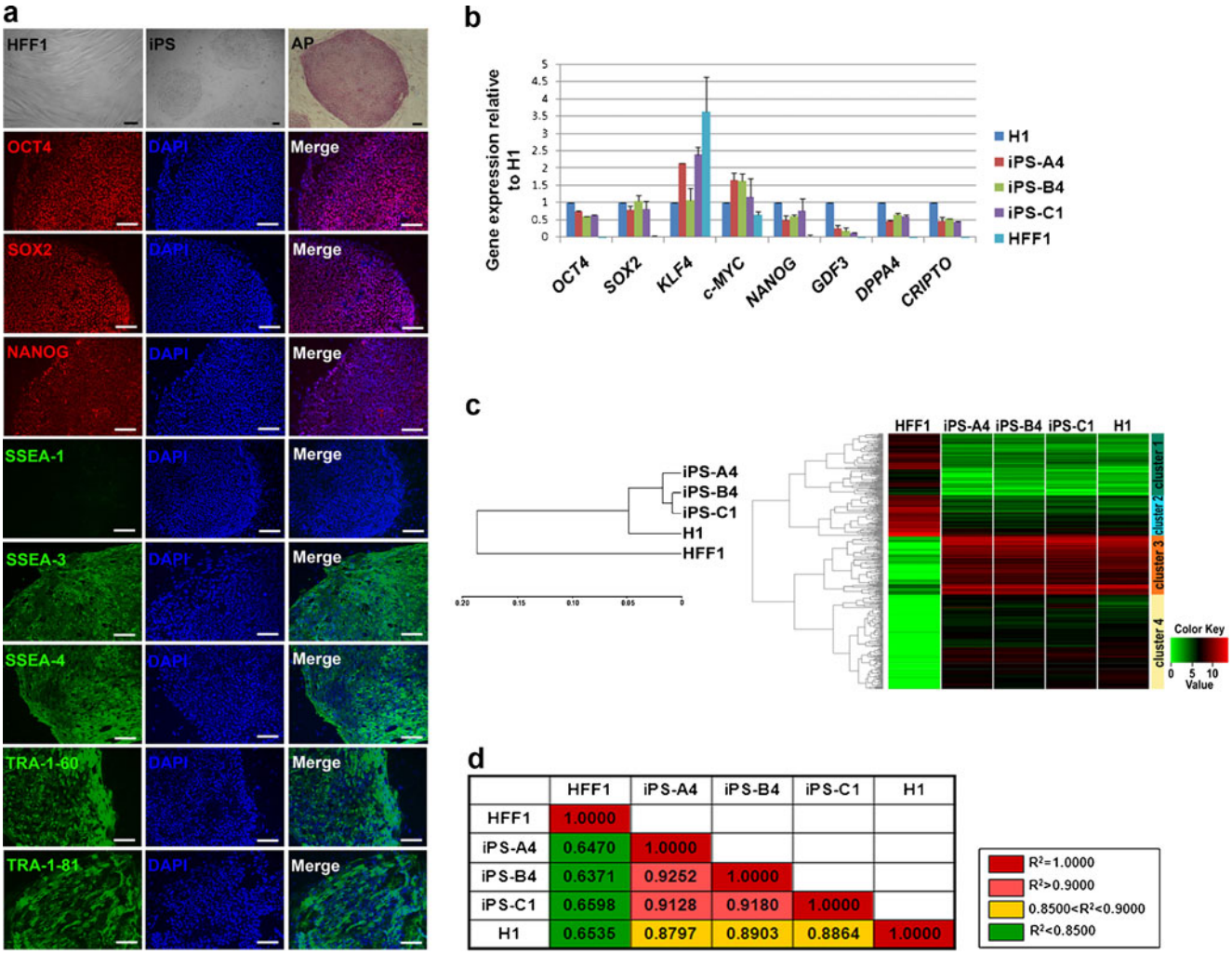

Fig. 2 iPS cells derived from 8-Br-cAMP-treated cells are similar to ES cells in expression of pluripotency markers and transcriptomes. **a** iPS cells derived from human embryonic foreskin fibroblast (HFF1) cells formed colonies with ES cell-like morphologies in co-culture with irradiated MEF feeder layers. Immunofluorescence analysis showed iPS cells express pluripotency markers, including alkaline phosphatase (AP), OCT4, SOX2, NANOG, SSEA-3, SSEA-4, TRA-1-60, and TRA-1-81, but not SSEA-1. Scale bars represent 100 μm. **b** Quantitative Real-Time PCR analysis of pluripotency-associated genes in HFF1, iPS, and H1 cells. Expression values were normalized over the expression of *GAPDH* and presented as relative changes compared to ES cells (H1). **c** Hierarchical cluster analysis (upper panel) and a heatmap (lower panel) of the transcriptomes of HFF1, iPS, and ES cells. Genes and samples were clustered by similar expression patterns using Euclidean distance measure. **d** Pearson correlation co-efficient of the entire expression data (Illumina microarrays) between indicated cell types

immunofluorescence staining of proteins defining these lineages (Fig. 3a). To test differentiation potential *in vivo*, we subcutaneously injected iPS cells into immunodeficient mice. After two months, we observed the generation of tumors (Fig. 3b). The tumors were dissected, sectioned and stained with hematoxylin and eosin. These results confirmed that iPS-A4 and iPS-B4 differentiated into representative tissues of the three embryonic germ layers (Fig. 3c and Supplemental Fig. S5). In contrast, iPS-C1 formed a cystic teratoma with evidence of gut-like epithelium (endoderm), spindle shaped stroma (mesoderm), and tubular epithelium (endoderm). This is shown in Supplemental Fig. S5.

Downstream Targets of 8-Br-cAMP and VPA

Four factor-transduced HFF1 cells were supplemented with 0.1 mM 8-Br-cAMP, 0.5 mM VPA or both in duplicate for 1 and 7 days respectively followed by microarray-based transcriptome analysis (four factor-transduced HFF1 cells without supplementation served as control cells). As shown in Fig. 4a, hierarchical clustering analysis revealed that the transcriptomes of 8-Br-cAMP-treated cells resemble that of control cells, whilst 8-Br-cAMP+VPA-treated cells clustered together with VPA-treated cells at day 1 of treatment. At day 7 of treatment, the transcriptomes of VPA-treated cells were closer to that of control cells, whilst 8-Br-cAMP+VPA-treated cells

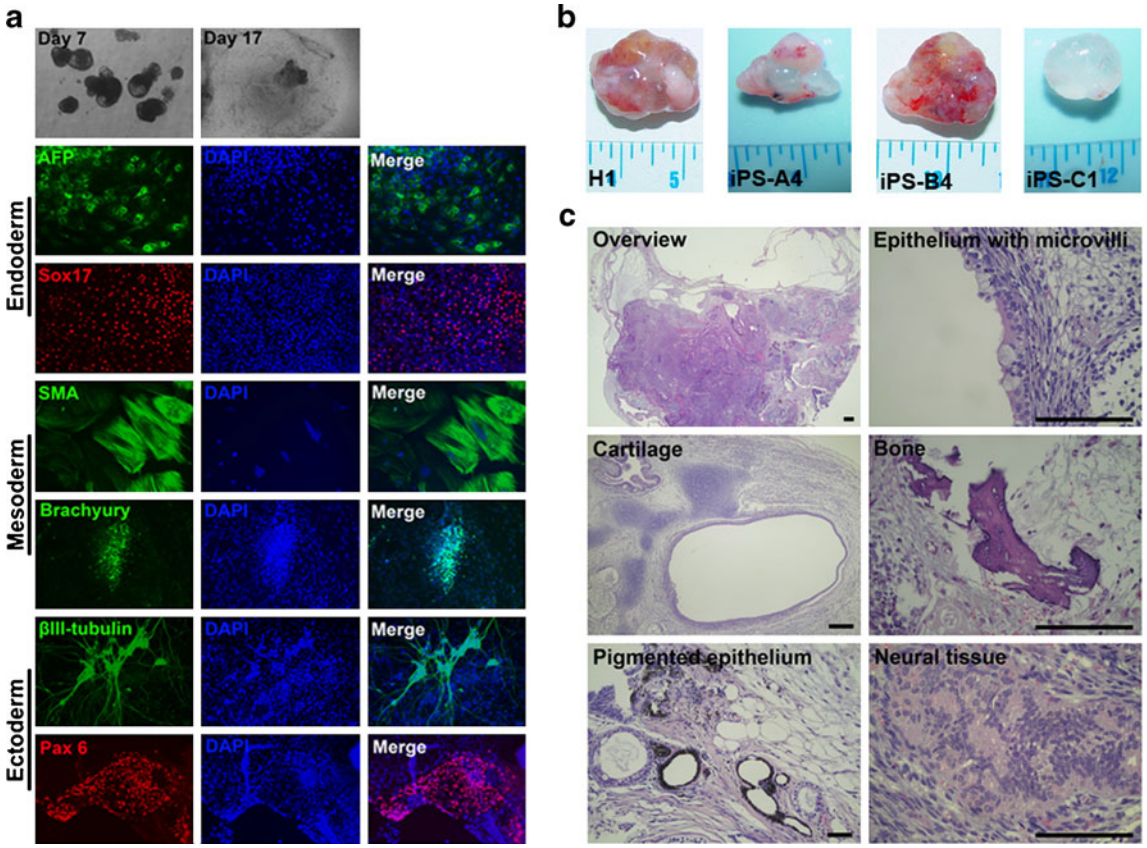

Fig. 3 Demonstration of pluripotency *in vitro* and *in vivo*. **a** After 7 days in suspension culture, iPS cells formed EBs and were then re-plated onto gelatin-coated dishes. After 10 days, attached cells showed distinct types of morphologies. Scale bars represent 200 μm. Immunofluorescence staining confirmed iPS cells differentiated into endoderm: α-FETOPROTEIN (AFP), SOX17; mesoderm: α-SMOOTH MUSCLE ACTIN (SMA), BRACHYURY; and ectoderm: βIII-TUBULIN, PAX6. Scale bars represent 50 μm. **b** Human iPS cells were subcutaneously injected into immunodeficient mice and formed teratomas. **c** Hematoxylin-eosin (H&E) staining of teratoma sections derived from iPS-A4 and iPS-B4 illustrate tissues representing all three embryonic germ layers. Endoderm: epithelium with microvilli; mesoderm: cartilage tissue, bone; ectoderm: pigmented epithelium, neural tissue. All of the images are representative sections from all the dissected teratomas. In contrast, iPS-C1 formed a cystic teratoma with gut-like epithelium (endoderm), spindle shaped stroma (mesoderm), and tubular epithelial structure (endoderm). The *in vivo* differentiation potential of the three iPS cell lines are elaborated in Supplemental Fig. S5. Scale bars represent 100 μm

clustered together with 8-Br-cAMP-treated cells. These cells were still at an early reprogramming stage, similar to HFF1 cells, and distinct from iPS and ES cells. We then evaluated the distinct and overlapping transcriptional signatures in (i) 8-Br-cAMP-treated cells, control cells, and ES cells, (ii) VPA-treated cells, control cells, and ES cells, (iii) 8-Br-cAMP +VPA-treated cells, control cells, and ES cells based on expression P values <0.01 (Supplemental Fig. S6, Supplemental Table S2, and Supplemental Table S3). The transcriptomes of 8-Br-cAMP+VPA-treated cells were more similar to ES cells, as indicated by the higher number of unique overlap between 8-Br-cAMP+VPA-treated cells and ES cells (day 1 of treatment: 248 genes; day 7 of treatment: 252 genes) than those between 8-Br-cAMP-treated cells and ES cells (day 1 of treatment: 185 genes, for example, *CCNE1*, *CCNB1IP1*-cyclin B1 interacting protein 1, *CCNDBP1*-cyclin D-type binding-protein 1; day 7 of treatment: 175 genes, for example, pluripotency asscociated genes-*DPPA3*, *DPPA5*, and *CCNH*,) or between VPA-treated cells and ES cells (day 1 of treatment: 219 genes; day 7 of treatment: 251 genes).

We further performed DAVID pathway analysis for comparison between the distinct small molecule-treated cells and control cells. The up-regulated pathways at day 1 of treatment include cytokine-related and inflammatory pathways. Besides these pathways, the combination of 8-Br-cAMP and VPA down-regulated several genes and pathways, including p53 (*CDC2, CCNB2, GTSE1*, *SERPINE1*), cell cycle (*CDC2, PLK1, WEE1*, *CCNB2*), CDC25 (*WEE1*, *CDC2*), and RB (*WEE1*, *CDC2*) pathways (Supplemental Table S4). At day 7 of treatment, the combination of 8-Br-cAMP and VPA induced up-regulation of the self-renewal supporting cyclin-encoding gene *CCND2* and associated *CCNA1* and *CCNE1* (Supplemental Table S5).

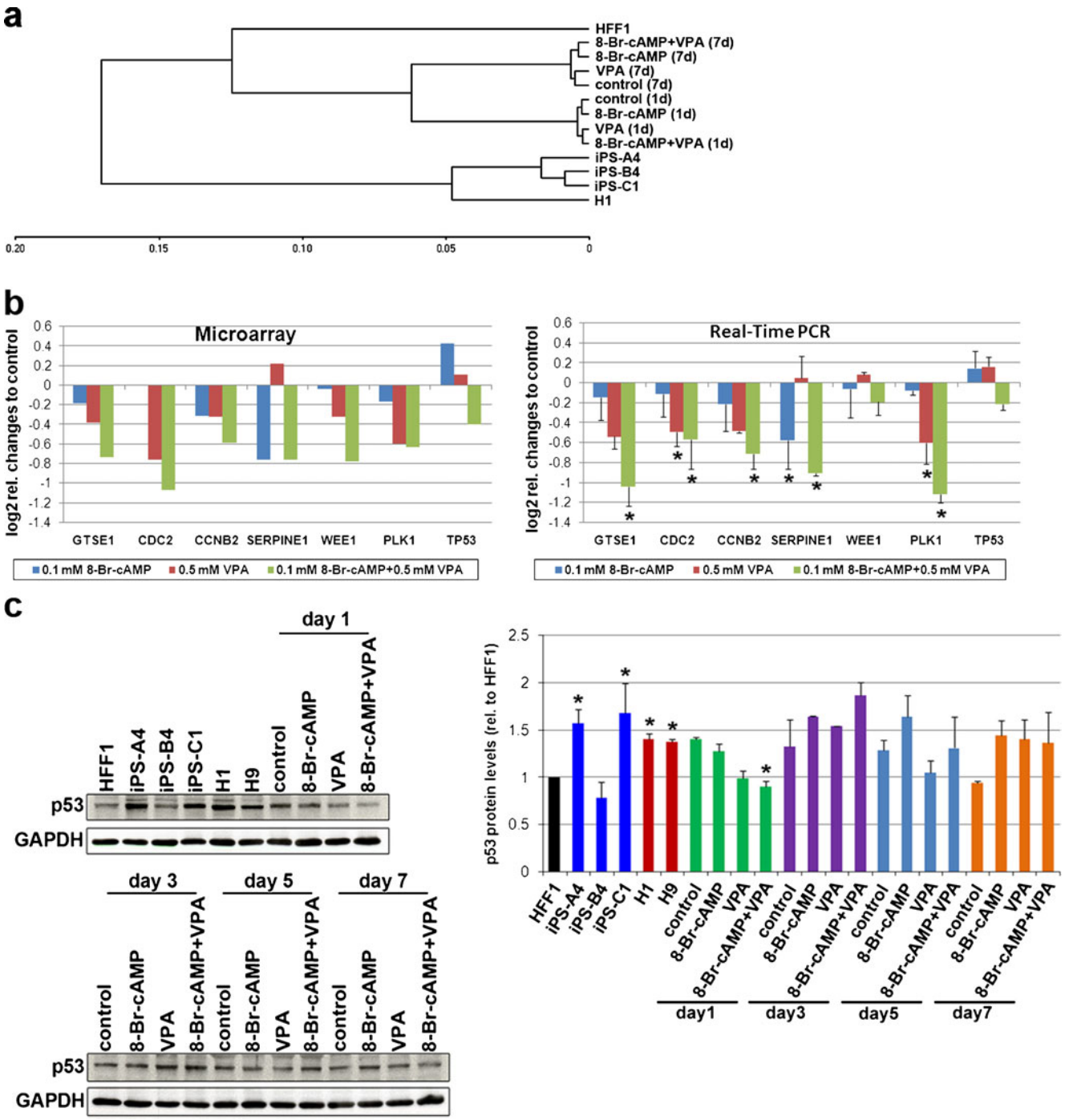

Fig. 4 Downstream targets of 8-Br-cAMP and VPA. **a** Hierarchical clustering of global gene-expression data of the indicated samples. Genes and samples were clustered by similar expression patterns using Euclidean distance measure. **b** Quantitative Real-Time PCR validations of the microarray data. The expression of *GTSE1*, *CDC2*, *CCNB2*, *SERPINE1*, *WEE1*, *PLK1,* and *TP53* was detected at day 1 of treatment in duplicate. Expression values were normalized over the expression of *GAPDH* and presented as relative changes compared to control cells. **c** Western blot showing expression levels of p53 in HFF1, iPS, ES, and four factor-transduced HFF1 cells treated with the indicated small molecules at day 1, 3, 5, 7 of treatment in duplicate. Expression values were normalized over the expression of GAPDH and presented as relative changes compared to HFF1 cells. *P* values <0.05 are indicated by an asterisk. iPS-A4 versus HFF1, iPS-C1 versus HFF1, H1 versus HFF1, H9 versus HFF1, 8-Br-cAMP+VPA-treated cells (day 1 of treatment) versus control cells

Subsequently, we independently verified the expression levels of the genes (day 1 of treatment) down-regulated in the following pathways: p53 (*GTSE1, CDC2, CCNB2*, *SERPINE1*), cell cycle (*CDC2, PLK1, WEE1*, *CCNB2*), and CDC25 (*WEE1*, *CDC2*), RB (*WEE1*, *CDC2*) by quantitative Real-Time PCR (Fig. 4b). The combination of 8-Br-cAMP and VPA down-regulated the expression levels of *GTSE1*, *CCNB2*, *SERPINE1*, and *PLK1*. In addition, the transcript expression level of *TP53* in the 8-Br-cAMP +VPA-treated cells was slightly lower than that of control cells. Furthermore, we analyzed the protein expression levels of p53 in HFF1, iPS, ES cells, and four factor-transduced HFF1 cells treated with the small molecules in duplicate. The expression level of p53 decreased in the 8-Br-cAMP+VPA-treated cells as compared to control cells at day 1 of treatment, and was comparable to that of control cells at days 3, 5, and 7 of treatment (Fig. 4c). The expression levels of p53 in iPS-A4 and iPS-C1 cells were similar to those of H1 and H9 cells, and higher than that of HFF1 cells. Nevertheless, the expression level of p53 in iPS-B4 was similar to that of HFF1 cells.

Discussion

We have demonstrated that 0.1/0.5 mM 8-Br-cAMP can enhance the reprogramming efficiency (2-fold) of HFF1 cells transduced with the four transcription factors, namely OCT4, SOX2, KLF4, and c-MYC. In addition, the combination of 0.1 mM 8-Br-cAMP and 0.5 mM VPA had a synergistic effect on improving the reprogramming efficiency to 6.5-fold. However, the combination of 0.5 mM 8-Br-cAMP and 0.5 mM VPA did not significantly increase the number of NANOG positive ES cell-like colonies like the combination of 0.1 mM 8-Br-cAMP and 0.5 mM VPA. A probable explanation for this is the cytotoxic effects resulting from higher doses of these two small molecules. iPS cells derived from 8-Br-cAMP-treated cells are similar to human ES cells not only in morphology, but also in the expression of pluripotency markers, karyotype, transcriptomes and differentiation potential (*in vitro* and *in vivo*).

8-Br-cAMP, a brominated derivative of cyclic AMP, is an activator of cyclic AMP-dependent protein kinase (PKA) [35]. It has been shown to inhibit proliferation, induce differentiation and apoptosis in a malignant glioma cell line (A-172) and an esophageal cancer cell line (Eca-109) [36, 37]. Modulation of the cAMP/PKA pathway may thus represent a possible target site for treating malignant tumors and 8-Br-cAMP meets this criteria in a clinical setting. In contrast to the anti-proliferative and apoptotic effects of 8-Br-cAMP in cancer cell lines, in our reprogramming protocol 8-Br-cAMP does not induce these effects (Supplemental Fig. S2).

In 2008, Huangfu et al. reported that VPA could increase the number of human ES cell-like colonies induced with 3 factors (OCT4, SOX2, and KLF4) by 10- to 20-fold [24]. However, in our case we only observed a 3-fold increase in the number of NANOG positive ES cell-like colonies induced with 4 factors under VPA supplementation. Possible explanations for these differences in the effect of VPA are as follows.

First, Huangfu et al. conducted their experiment with 3 factors. In contrast, we transduced 4 factors (OCT4, SOX2, KLF4, and c-MYC) into HFF1 cells. The efficiencies of viral infection are different in the both conditions. Secondly, Huangfu *et al*. induced BJ (neonatal human foreskin fibroblasts) and NHDF (normal neonatal human dermal fibroblasts) into iPS cells, while we used HFF1 (human foreskin fibroblasts) cells. It is probable that the different cell types respond differently to VPA. In addition, Warren *et al.* recently successfully induced pluripotency in several somatic cells, including Detroit 551, BJ, CF (fibroblast-like cells cultured from a primary skin biopsy taken from an adult cystic fibrosis patient) and MRC-5 fetal fibroblasts using *in vitro* derived RNA encoding *OCT4, SOX2, KLF4, c-MYC,* and *LIN28* [38]. They also supplemented their medium with VPA, however, this did not have a significant effect on the reprogramming efficiency. Our findings together with that of Warren et al. [38] would suggest that the effect (magnitude of efficiency) of VPA on cellular reprogramming might be cell type and laboratory-dependent.

To facilitate our understanding of the mechanisms underlying the observed increase in reprogramming efficiency, four factor-transduced HFF1 cells were in duplicate supplemented with 0.1 mM 8-Br-cAMP, 0.5 mM VPA or both for 1 and 7 days respectively, followed by microarray-based transcriptome analysis. These two time points were chosen in order to identify early immediate direct (day 1 of treatment) and indirect (day 7 of treatment) target genes and their associated signaling pathways.

The significance of up-regulated cytokine-related and inflammatory pathways is unknown. Nonetheless, we cannot exclude the possibility that the increased cytokine-related and inflammatory pathways could be an immune response to the viral infection of the HFF1 cells. Interestingly, it has also been demonstrated that anti-inflammatory drugs can promote self-renewal in human ES cells [39]. Besides these genes and pathways, the combination of 8-Br-cAMP and VPA down-regulated additional genes and pathways, including p53 (*CCNB2, GTSE1*, *SERPINE1*) and cell cycle (*PLK1, CCNB2*) pathways. At day 7 of treatment time point, 8-Br-cAMP and VPA induced up-regulation of *CCND2*, *CCNA1* and *CCNE1*. The effect of *CCNA1, CCND2*, and *CCNE1* on cellular reprogramming is unknown. However, it has been shown that *CCND2* which encodes CYCLIN D2 is required for maintaining self-renewal in human ES cells [40].

Remarkably, the combination of 8-Br-cAMP and VPA induced a transient decrease in the protein expression level of p53 during the early stages of reprogramming. Coincidentally, there were six independent reports suggesting that siRNA-mediated ablation of p53 function significantly increases the efficiency of inducing pluripotency in somatic cells [27–32].

The transcription factor p53 (the protein encoded by the *TP53* gene) functions as a tumor suppressor preventing cancer, partly by safeguarding genome stability by promoting senescence in DNA damaged cells. Intriguingly, the combination of 8-Br-cAMP and VPA only suppressed the protein levels of p53 during the early stages of reprogramming. In this respect, this combination has an advantage over siRNA-p53 or vitamin C-mediated reprogramming, which persistently down-regulate p53 protein levels [22, 27–32].

Additionally, we are currently screening for other small molecules that might ultimately enable the induction of pluripotency in somatic cells without disabling mechanisms that safeguard genome integrity.

Acknowledgments This work was supported by the Max Planck Society and the BMBF Initiative "Medizinischen Systembiologie—MedSys" (DRUG-iPS/ 0315398G) to YW and JA. The authors would like to thank all colleagues in the Adjaye lab for support and fruitful discussions, A. Wulf-Goldenberg for the teratoma assay, and A. Sabha at the microarray facility.

Disclosures The authors indicate no potential conflicts of interest.

Author Contributions Y.W. conceived the experiments, performed the experiments, and wrote the manuscript. J.A. conceived the experiments, and wrote the manuscript.

References

1. Takahashi, K., & Yamanaka, S. (2006). Induction of pluripotent stem cells from mouse embryonic and adult fibroblast cultures by defined factors. *Cell, 126*(4), 663–676.
2. Meissner, A., Wernig, M., & Jaenisch, R. (2007). Direct reprogramming of genetically unmodified fibroblasts into pluripotent stem cells. *Nat Biotechnol, 25*(10), 1177–1181.
3. Takahashi, K., Tanabe, K., Ohnuki, M., et al. (2007). Induction of pluripotent stem cells from adult human fibroblasts by defined factors. *Cell, 131*(5), 861–872.
4. Yu, J., Vodyanik, M. A., Smuga-Otto, K., et al. (2007). Induced pluripotent stem cell lines derived from human somatic cells. *Science, 318*(5858), 1917–1920.
5. Dimos, J. T., Rodolfa, K. T., Niakan, K. K., et al. (2008). Induced pluripotent stem cells generated from patients with ALS can be differentiated into motor neurons. *Science, 321* (5893), 1218–1221.
6. Park, I. H., Arora, N., Huo, H., et al. (2008). Disease-specific induced pluripotent stem cells. *Cell, 134*(5), 877–886.
7. Ebert, A. D., Yu, J., Rose, F. F., Jr., et al. (2009). Induced pluripotent stem cells from a spinal muscular atrophy patient. *Nature, 457*(7227), 277–280.
8. Soldner, F., Hockemeyer, D., Beard, C., et al. (2009). Parkinson's disease patient-derived induced pluripotent stem cells free of viral reprogramming factors. *Cell, 136*(5), 964–977.
9. Raya, A., Rodríguez-Pizà, I., Guenechea, G., et al. (2009). Disease-corrected haematopoietic progenitors from Fanconi anaemia induced pluripotent stem cells. *Nature, 460*(7251), 53–59.
10. Song, Z., Cai, J., Liu, Y., et al. (2009). Efficient generation of hepatocyte-like cells from human induced pluripotent stem cells. *Cell Res, 19*(11), 1233–1242.
11. Si-Tayeb, K., Noto, F. K., Nagaoka, M., et al. (2010). Highly efficient generation of human hepatocyte-like cells from induced pluripotent stem cells. *Hepatology, 51*(1), 297–305.
12. Sullivan, G. J., Hay, D. C., Park, I. H., et al. (2010). Generation of functional human hepatic endoderm from human induced pluripotent stem cells. *Hepatology, 51*(1), 329–335.
13. Zhang, J., Wilson, G. F., Soerens, A. G., et al. (2009). Functional cardiomyocytes derived from human induced pluripotent stem cells. *Circ Res, 104*(4), e30–e41.
14. Zhang, D., Jiang, W., Liu, M., et al. (2009). Highly efficient differentiation of human ES cells and iPS cells into mature pancreatic insulin-producing cells. *Cell Res, 19*(4), 429–438.
15. Choi, K. D., Yu, J., Smuga-Otto, K., et al. (2009). Hematopoietic and endothelial differentiation of human induced pluripotent stem cells. *Stem Cells, 27*(3), 559–567.
16. Taura, D., Noguchi, M., Sone, M., et al. (2009). Adipogenic differentiation of human induced pluripotent stem cells: Comparison with that of human embryonic stem cells. *FEBS Lett, 583*(6), 1029–1033.
17. Chambers, S. M., Fasano, C. A., Papapetrou, E. P., Tomishima, M., Sadelain, M., & Studer, L. (2009). Highly efficient neural conversion of human ES and iPS cells by dual inhibition of SMAD signaling. *Nat Biotechnol, 27*(3), 275–280.
18. Mikkelsen, T. S., Hanna, J., Zhang, X., et al. (2008). Dissecting direct reprogramming through integrative genomic analysis. *Nature, 454*(7200), 49–55.
19. Huangfu, D., Maehr, R., Guo, W., et al. (2008). Induction of pluripotent stem cells by defined factors is greatly improved by small-molecule compounds. *Nat Biotechnol, 26*(7), 795–797.
20. Shi, Y., Desponts, C., Do, J. T., Hahm, H. S., Schöler, H. R., & Ding, S. (2008). Induction of pluripotent stem cells from mouse embryonic fibroblasts by Oct4 and Klf4 with small-molecule compounds. *Cell Stem Cell, 3*(5), 568–574.
21. Shi, Y., Do, J. T., Desponts, C., Hahm, H. S., Schöler, H. R., & Ding, S. (2008). A combined chemical and genetic approach for the generation of induced pluripotent stem cells. *Cell Stem Cell, 2* (6), 525–528.
22. Esteban, M. A., Wang, T., Qin, B., et al. (2010). Vitamin C enhances the generation of mouse and human induced pluripotent stem cells. *Cell Stem Cell, 6*(1), 71–79.
23. Wang, Y., Mah, N., Prigione, A., Wolfrum, K., Andrade-Navarro, M. A., & Adjaye, J. (2010). A transcriptional roadmap to the induction of pluripotency in somatic cells. *Stem Cell Rev, 6*(2), 282–296.
24. Huangfu, D., Osafune, K., Maehr, R., et al. (2008). Induction of pluripotent stem cells from primary human fibroblasts with only Oct4 and Sox2. *Nat Biotechnol, 26*(11), 1269–1275.
25. Lin, T., Ambasudhan, R., Yuan, X., et al. (2009). A chemical platform for improved induction of human iPSCs. *Nat Methods, 6* (11), 805–808.
26. Babaie, Y., Herwig, R., Greber, B., et al. (2007). Analysis of Oct4-dependent transcriptional networks regulating self-renewal and pluripotency in human embryonic stem cells. *Stem Cells, 25*(2), 500–510.
27. Zhao, Y., Yin, X., Qin, H., et al. (2008). Two supporting factors greatly improve the efficiency of human iPSC generation. *Cell Stem Cell, 3*(5), 475–479.

28. Hong, H., Takahashi, K., Ichisaka, T., et al. (2009). Suppression of induced pluripotent stem cell generation by the p53-p21 pathway. *Nature, 460*(7259), 1132–1135.
29. Li, H., Collado, M., Villasante, A., et al. (2009). The Ink4/Arf locus is a barrier for iPS cell reprogramming. *Nature, 460*(7259), 1136–1139.
30. Kawamura, T., Suzuki, J., Wang, Y. V., et al. (2009). Linking the p53 tumour suppressor pathway to somatic cell reprogramming. *Nature, 460*(7259), 1140–1144.
31. Utikal, J., Polo, J. M., Stadtfeld, M., et al. (2009). Immortalization eliminates a roadblock during cellular reprogramming into iPS cells. *Nature, 460*(7259), 1145–1148.
32. Marión, R. M., Strati, K., Li, H., et al. (2009). A p53-mediated DNA damage response limits reprogramming to ensure iPS cell genomic integrity. *Nature, 460*(7259), 1149–1153.
33. Park, I. H., Zhao, R., West, J. A., et al. (2008). Reprogramming of human somatic cells to pluripotency with defined factors. *Nature, 451*(7175), 141–146.
34. Prigione, A., Fauler, B., Lurz, R., Lehrach, H., & Adjaye, J. (2010). The senescence-related mitochondrial/oxidative stress pathway is repressed in human induced pluripotent stem cells. *Stem Cells, 28*(4), 721–733.
35. Ogreid, D., Ekanger, R., Suva, R. H., Miller, J. P., & Døskeland, S. O. (1989). Comparison of the two classes of binding sites (A and B) of type I and type II cyclic-AMP-dependent protein kinases by using cyclic nucleotide analogs. *Eur J Biochem, 181*(1), 19–31.
36. Chen, T. C., Hinton, D. R., Zidovetzki, R., & Hofman, F. M. (1998). Up-regulation of the cAMP/PKA pathway inhibits proliferation, induces differentiation, and leads to apoptosis in malignant gliomas. *Lab Invest, 78*(2), 165–174.
37. Wang, H. M., Zheng, N. G., Wu, J. L., Gong, C. C., & Wang, Y. L. (2005). Dual effects of 8-Br-cAMP on differentiation and apoptosis of human esophageal cancer cell line Eca-109. *World J Gastroenterol, 11*(41), 6538–6542.
38. Warren, L., Manos, P. D., Ahfeldt, T., et al. (2010). Highly efficient reprogramming to pluripotency and directed differentiation of human cells with synthetic modifed mRNA. Cell Stem Cell. [Epub ahead of print].
39. Desbordes, S. C., Placantonakis, D. G., Ciro, A., et al. (2008). High-throughput screening assay for the identification of compounds regulating self-renewal and differentiation in human embryonic stem cells. *Cell Stem Cell, 2*(6), 602–612.
40. Becker, K. A., Ghule, P. N., Lian, J. B., Stein, J. L., van Wijnen, A. J., & Stein, G. S. (2010). Cyclin D2 and the CDK substrate p220 (NPAT) are required for self-renewal of human embryonic stem cells. *J Cell Physiol, 222*(2), 456–464.